

Compressor Map Prediction by Neural Networks

Thomas Palmé¹, Phillip Waniczek², Herwart Hönen², Mohsen Assadi¹ and Peter Jeschke²

1. Department of Mechanical and Structural Engineering and Material Science, University of Stavanger, Stavanger N-4036, Norway

2. Institute of Jet Propulsion and Turbomachinery, RWTH Aachen University, Aachen 52062, Germany

Received: September 25, 2011 / Accepted: January 05, 2012 / Published: October 31, 2012.

Abstract: This paper presents a study where artificial neural networks are used as a curve fitting method applying measured data from an axial compressor test rig to predict the compressor map. Emphasis is on models for prediction of pressure ratio, compressor mass flow and mechanical efficiency. Except for evaluation of interpolation and extrapolation capabilities, this study also investigates the effect of the design parameters such as number of neurons and size of training data. To reduce the effect of noise, the auto associative neural network has been applied for noise filtering of the data from the parameters used to calculate the efficiency. In summary, the results show that artificial neural network can be used for compressor map prediction, but it should be emphasized that the selection of data normalisation scale is crucial for the model where compressor mass flow is predicted. Furthermore, it is shown that the AANN (auto associative neural network) can be used to reduce noise in measured data and thereby enhance the quality of the data.

Key words: Axial flow compressor, artificial neural networks, curve fitting, noise reduction.

Nomenclature

c_p	Heat capacity
m	Mass flow rate
Dif	Measurement pane at compressor exit (diffuser)
Inl	Measurement plane at compressor inlet
P	Power
R	Rotor/gas constant
S	Stator
T	Temperature (K)
V	Volume flow
p	Pressure
κ	Isentropic exponent
ρ	Density
t	Total
ANN	Artificial neural network
AANN	Auto associative neural network
GRN	General regression networks
MLP	Multi layer perceptrons
NN	Neural networks
RBF	Radial basis function

1. Introduction

Simulation of gas turbines is important for design and test of gas turbine control strategies and requires

Corresponding author: Mohsen Assadi, professor, research fields: system analysis, energy conversion, monitoring, emission reduction. E-mail: mohsen.assadi@uis.no.

accurate models of the gas turbine components. The compressor is a critical part of the overall model and detailed models that incorporate the compressor characteristics are therefore required. In the simplest form, the compressor characteristics can be implemented in a table form but this is not well suited for engine simulation since the standard interpolation routines is not continuously differentiable. The compressor characteristics are expressed by the relationship between the pressure ratio π^* , corrected speed $n_c/\sqrt{T_1^*}$, corrected mass flow rate $m_c\sqrt{T_1^*/p_1^*}$ and efficiency η_c^* , where the interrelationships between the variables normally are referred to the compressor map which can be derived from the Buckingham theorem. The pressure ratio, corrected speed and corrected mass flow are parameters that can be physically measured while the efficiencies are so-called independent parameters which are calculated values using measured parameters. There are several different methods to approximate the compressor characteristics, or the compressor map, one is e.g. a two-dimensional linear interpolation as shown in Ref. [1]. In Ref. [2], a

generalized procedure for analytical compressor map prediction is outlined and later applied and presented in Ref. [3]. In Ref. [4], auxiliary coordinates were introduced which were superimposed on the characteristic curves to obtain the compressor characteristics. In Ref. [5], the authors applied analytical functions to nonlinear models to approximate the compressor map of different designs. Another approach was taken in Refs. [6, 7] applying genetic algorithms in performance model calculations and analytical functions for compressor map generation. Several studies such as Refs. [1, 8-11] have evaluated different neural networks for compressor map generation. In Ref. [11], the authors showed that the MLP (multi layer perceptron) when compared to RBFs (radial basis function networks), GRNs (general regression networks) and rotated general regression network is the most suitable neural network model to implement due to the high interpolation capability, but rather complicated networks were used with two hidden layers with 10 neurons in each layer, corresponding to a rather complex network structure. Application of neural network models is in addition evaluated in Ref. [8], where good results are obtained for compressor pressure ratio prediction while the ANN (artificial neural network) fails to predict the compressor mass flow, instead an analytical approach was adopted for mass flow prediction. Even though several studies report the application of ANN for compressor performance modelling, the existing literature does not provide an answer of how to develop and configure these models in an optimal manner as well as quantifying the number of required data points from the compressor map.

The AANN (auto associative neural network) was originally proposed by Kramer [12] to deal with data filtering and sensor validation through nonlinear principal component analysis. Basically, this ANN model replicates the input at the output, under the constraint of a reduced dimension inside the model. By the virtue of the reduced dimension, the network is

forced to compress the data into a lower dimension and thereby account for interrelationships between the parameters and discard the noise which should be uncorrelated between the parameters. Applications of AANN for noise-filtering from nonlinear correlated parameters can be found in e.g. Ref. [13], where it was used to improve the failure diagnostic capability of the gas path analysis method.

In this study, ANNs will be used as a curve fitting method to approximate the compressor map. Three different compressor map models will be considered where the first predicts the pressure ratio, the second predicts the mass flow while the third model predicts the mechanical efficiency. These models are developed by applying measured data from an axial compressor research test rig. It will be shown that the ANN models can be developed by rather few data points from the compressor map and that interpolation results are excellent. In addition, it will be seen that extrapolation outside the training domain can be performed, but at reduced accuracy. Furthermore, it will be shown that the model for mass flow prediction requires an unconventional data normalisation which is due to almost vertical speed lines in this model. Noise reduction capability by the AANN will be investigated on the data used for mechanical efficiency calculation, and the results show that the calculated efficiency becomes less scattered when the data has been processed through an AANN. The result in this study is based on a data set from one compressor, but the modelling results can be considered as generic and be useful for curve fitting of data from other compressors with similar characteristics.

2. The Compressor Test Rig

The two stage axial flow compressor of the Institute of Jet Propulsion and Turbo Machinery of the University of Aachen is specially designed for the investigation of the effects of axial spacing on performance and compressor flow field [14]. Beside the complex design of the rig, giving the opportunity to

vary the axial spacing, a second major task is to equip the rig with measurement technique that is capable to resolve the minimal differences of the flow field caused by the variation of the axial gap. Hence, the measurement equipment used must have high measurement accuracy. A schematic illustration of the test rig is shown in Fig. 1. For calculating the performance data of the test rig, total temperature, total pressure and mass flow measurements are used mainly. For that purpose, the inlet and exit of the compressor is equipped with an extensive measurement plane consisted of total pressure and temperature keel-probe-rakes. These keel-probes have a wide scale of incidence angle of $\pm 25^\circ$. In the inlet of the compressor (plane Inl in Fig. 1), there are four probe-rakes located around the circumference having a circumferential distance of 90° between each other. Each rake has three total pressure and one total temperature measurement position on different channel heights. The radial position of all measurement positions is determined by a method of centroidal axis and result in a higher density of measurement locations at the hub and tip. In total, the four rakes allocate 12 total pressure and four total temperature measurement positions around the circumference in the inlet of the compressor rig. The exit measurement plane (Dif) is located 275 mm behind stator 2 (referring to nominal

axial gap) and consists of five rakes equally distributed circumferentially. These keel-probe rakes are designed a little bit different from the ones located in the inlet. For increasing the density of measurement positions, each rake is manufactured as a twin rake. One rake consists of five total pressure and five total temperature measurement positions spread radially. In total, the exit plane is equipped by a matrix of $5 \times 5 (= 25)$ total pressure and total temperature measurement positions. For performance evaluation, the pressure and temperature values are arithmetically averaged but also logged as single values.

The mass flow rate of the compressor is calculated from a calibrated venturi nozzle and a density determination. Density is calculated by two combined total pressure and total temperature probes and static wall pressure upstream of the nozzle. The venturi nozzle is used for deriving the volume flow by measuring the differential pressure. For increasing of the accuracy, the static pressure of the venturi nozzle is measured at four positions around the annulus, which are physically averaged by a triple T-arrangement. The differential pressure is measured twice, by a more accurate mensor and by a psi module for reference. In order to calculate the mechanical efficiency friction losses in the bearings are determined by the temperature difference of the oil inflow and outflow.

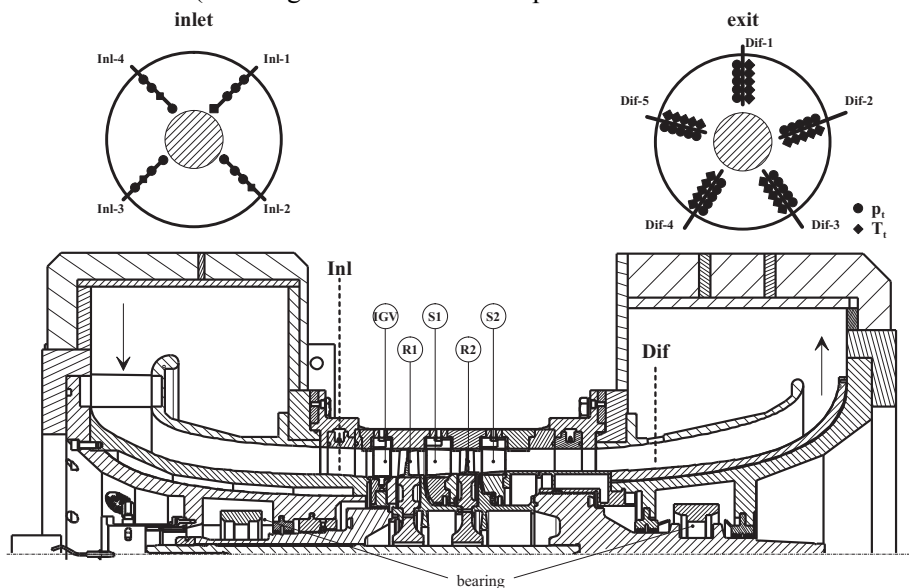


Fig. 1 Cross-sectional view of the axial compressor including the measurement planes.

The temperatures are measured with Pt100. The drive power of the electric motor is measured by a torque meter. The thermal efficiency is calculated by the total temperature and total pressure measurements of the inlet and exit planes. The compressor is operated in a closed loop. At design speed, it delivers a mass flow rate of 7.7 kg/s and a pressure ratio of 1.67. During operation, the inlet pressure and temperature as well as the mechanical speed are remained constant. A more detailed description of the whole test facility is given by Ernst, et al. [15].

3. Measurement Accuracy and Data Set

As described earlier in this paper, performance data of the compressor are used to train neural networks. For that purpose, performance data, mainly total pressure ratio and mechanical efficiency are derived from keal-probe-rakes in the inlet and exit of the compressor. Table 1 summarizes the measurement accuracy of measurement locations, which are important in the study. The uncertainty in the calculation of the efficiency based on the measured data is described by:

$$\Delta f = \sqrt{\left(\frac{\partial f}{\partial x_1} \Delta x_1\right)^2 + \left(\frac{\partial f}{\partial x_2} \Delta x_2\right)^2 + \dots + \left(\frac{\partial f}{\partial x_n} \Delta x_n\right)^2} \quad (1)$$

where f is the function such as in Eq. (2). Δx is the mean error of the mean value. Thus using f , a confidence interval can be calculated, in which the true efficiencies are located. Eq. (1) assumes independently and identically distributed zero-mean Gaussian random variables x . The measurement accuracies are given for the design point of the compressor. The higher accuracy of the temperature measurement in the exit of the compressor is due to the higher temperatures in this region of the engine. Eq. (2) shows how the mechanical efficiency is calculated. In contrast to the absolute measurement accuracy, the relative measurement accuracy does not consider systematic errors. This consideration is allowed if two different axial spacing are compared to each other using the same measurement equipment.

Table 1 Measurement accuracies of different measurement chains.

Measurement position	Accuracy (absolute) (%)	Accuracy (relative) (%)
1 Pressure rakes (inlet and exit)	0.05	0.05
2 Temperature rakes (inlet)	0.42	0.22
3 Temperature rakes (exit)	0.18	0.08
4 Total pressure ratio	0.02	0.02
5 Mass flow rate	0.37	0.02
6 Differential pressure venturi nozzle	0.01	0.01
7 Thermal efficiency	0.78	0.18

$$\eta_{\text{mech}} = \frac{c_p \cdot T_{\text{inl}} \cdot \dot{V}_{\text{Air}} \cdot \left(\left(\frac{p_{\text{Dif}}}{p_{\text{inl}}} \right)^{\frac{\kappa-1}{\kappa}} - 1 \right)}{R \cdot T \cdot (P - \dot{V}_{\text{Oil}} \cdot \Delta T_{\text{Oil}} \cdot c_{p_{\text{Oil}}} \cdot \rho_{\text{Oil}})} \quad (2)$$

Especially the efficiencies and determination of mass flow rate are affected by the systematic errors. For the training of the neural networks, a large data set is recorded in the whole area of the compressor map. In total, data are taken on six different speed lines (60%, 70%, 83%, 90%, 95% and 97%) throttling the compressor from choke until it surged. Therefore, the surge line is the last stable point before real surge occurred. On each speed line, the compressor is stabilized at approximately 50 discrete points and performance measurements are carried out.

4. MLPs (Multi-Layer Perceptrons)

Feed forward multi-layer perceptrons are universal nonlinear function approximators which imply that they are able to approximate general mappings from one finite dimensional space to another. The mathematical expression of a one hidden layer neural network becomes:

$$y_k(x) = \sigma \left(\sum_{j=0}^M w_{ji}^{(2)} h \left(\sum_{i=1}^D w_{ji}^{(1)} x_i + w_{j0}^{(1)} \right) + w_{k0}^{(2)} \right) \quad (3)$$

where D is number of inputs, M is number of neurons or basis functions and w is the different matrices and vectors containing the coefficients that are adjusted during training. Most importantly, MLPs perform function approximation in a very attractive and precise manner by using simple basis functions, normally represented by the tangent hyperbolic or the sigmoid

function, see h and σ in Eq. (3), where the numbers of basis functions are fixed for a given model configuration but the shape of the basis functions are adaptive during the training phase. The result is that a compact model with few adaptive parameters can be obtained for rather complicated mappings compared to other methods such as polynomials or RBFs where the shape of the basis functions are fixed. However, in contrast to polynomials and RBF, there is no closed form solution for calculation of the optimal weight values and instead an iterative optimisation algorithm is required which does not theoretically guarantee convergence. Because of this, several networks of the same configuration is normally trained with slightly different initial weight values. Configuration of a model for a specific set of data is reduced to deciding the number of basis functions in the model, performed by selection of number of neurons in the so-called hidden layer; see M in Eq. (3). Higher number of basis functions or hidden neurons increases the functional complexity that the network can approximate but also imply that more data are required to ensure generalisation. There is no theory available for a priori decision of the correct number of neurons. In practice, this is a trial and error problem where the goal is to have an accurate model prediction using as few neurons as possible.

A second application of MLPs, apart from function approximation, is nonlinear principal component analysis through a three hidden layer configuration including a so-called bottleneck layer with a reduced dimension. This type of network is a so-called auto associator, trained to recreate the measurement vectors at the output layer as closely as possible, in a least-square error sense over a set of training data patterns. The smaller dimension in the bottleneck layer forces the network to learn the systematic correlations in the data, while exclude the random variations that are due to measurement noise, which is possible since measurement noise is uncorrelated between the sensors. Use of MLPs as non-linear feature extraction was introduced by Kramer [12] and exemplified in e.g.

Ref. [13].

5. Modelling Approach

The compressor map is approximated by training MLPs to reproduce the compressor characteristics applying the measured data. This means that the compressor characteristics are inherently implemented without any assumptions. Three different configurations of the compressor map and one auto associative model for noise reduction will be considered and named as follows:

$$\text{Model-I: } \pi_c = f(\dot{m}_c, N_c)$$

$$\text{Model-II: } \dot{m}_c = f(\pi_c, N_c)$$

$$\text{Model-III: } \eta_{mech} = f(\pi_c, \dot{m}_c)$$

$$\text{Model-IV: } \eta_{mech} = f(\eta_{mech})$$

Models I-III are configured as regression models, i.e. models that predict an output based on inputs, while Model-IV is configured as an auto associative model, i.e. a model that replicates the input at the output. Each regression model is approximated by a one hidden layer MLP, using the measured data as input or output to the network. In Model-III, the mechanical efficiency is a predicted parameter, but since this parameter is calculated based on six measured parameters, it becomes affected by the systematic uncertainty in these measured parameters. Because of this, the measured parameters that are used to calculate the mechanical efficiency are processed through an AANN prior to calculation of the efficiency. The mechanical efficiency which is calculated with the AANN processed parameters is then used as the target parameter in Model-III. The configurations of the models are performed in a trial and error approach implemented by training several networks with different number of neurons in the hidden layers. In the regression task, the problem is condensed into deciding the size of number of neurons in the hidden layer, while in the data noise cleaning AANN task there are two variables to be decided, number of neurons on the mapping layer, which should be of the same size and number of neurons in the bottleneck layer. The number

of neurons should in all cases be selected as low as possible to ensure good generalization capabilities. The adjustable parameters, i.e. the network weights, are a direct function of the network weights and a thumb of rule is that there should be at least a few data patterns per weight value. Each model is trained using three different data sets, the training set which is used to numerically adjust the network weights, the CV set (cross validation), which is used to stop training prior to overtraining and finally a test which is used to evaluate the trained network's performance. During training, the network weights are adjusted in an iterative process where all training patterns are first presented to the network and the MSE (mean square error) is calculated. By applying the back propagation algorithm, it is possible to evaluate, which weights as well as in what direction these should be adjusted in order to decrease the MSE. Adjustments of the network weights can be done by several different optimization algorithms such as the gradient descent method. However, in this study, the Levenberg-Marquardt algorithm [16] is used which is a modification of the Gauss-Newton optimisation algorithm. The Levenberg-Marquardt algorithm is faster and less prone to get stuck in local minima's in the error space compared to the basic gradient descent algorithm. The learning process is repeated several steps, one step is called one iteration. When the learning algorithm has converged, i.e. additional iterations do not cause a decrease in the error, the optimisation procedure is stopped and the network weights are saved. Due to the possibility of being trapped in a local minimum, several training sessions are performed with different initial weight values where the best in terms of the lowest prediction error is used. Evaluation of the possibility to be trapped in a local minimum can be done by comparing the training results for the different training sessions; big difference in terms of prediction accuracy indicates that the model is sensitive to the initial weight values and additional training sessions might be motivated.

6. Modelling Results

6.1 Predicted Pressure Ratio— $\pi_c = f(\dot{m}_c, N_c)$

The compressor map, according to Model-I, is trained with 206 data patterns from all speed lines. Of these 206 data patterns, 60% is used in the training set, 20% in cross validation set and the remaining 20% in the test set. The data is linearly rescaled between ± 0.8 prior to network training to allow for extrapolation of the data. The number of neurons represents in some sense the complexity between input and output parameters, and in this model it can be recognized in Fig. 2 that three neurons are enough to approximate the functional complexity between the input and output parameters. Three neurons in the hidden layer imply that 13 weights are used in the network configuration, which gives a data pattern per weight ratio of 9.5, only counting the data patterns in the training data set, which should be enough to avoid any over-fitting in the network. The training phase requires a few hundred iterations to converge, see Fig. 3 for the model with three hidden neurons.

To evaluate the interpolation capability, the network with three neurons in the hidden layer is retrained where one speed line between 97% and 60% is removed from the training data set at the time. The networks are then tested with the speed lines not used during training which is termed interpolation since this unseen speed lines during training is located inside the training data boundary. Fig. 4 shows the graphical result for speed line 95%, and in Table 2 a comparison between the interpolation error and training error for the four speed lines located between the lowest speed, 60%, and the highest, 97%, is shown. Table 2 shows that the interpolation capability is excellent, since the difference in error is almost indistinguishable between the cases where the speed line data are used during training and in the case where it is not seen at all. To investigate the extrapolation capability, a neural network with three hidden neurons was trained with all speed-lines except 60% and 97%, respectively. The

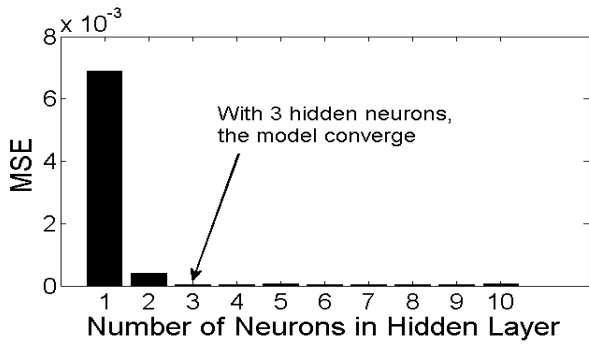


Fig. 2 MSE as a function of hidden neurons.

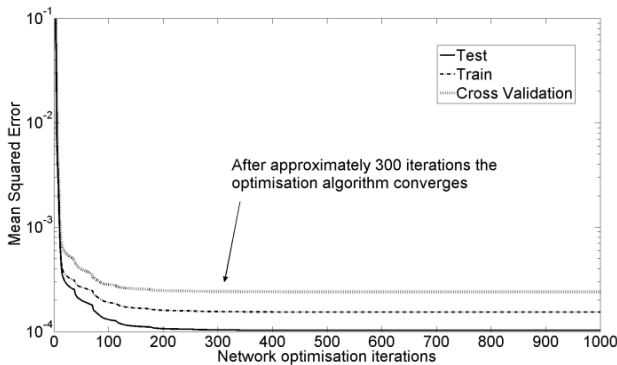


Fig. 3 Optimisation convergence with three hidden neurons.

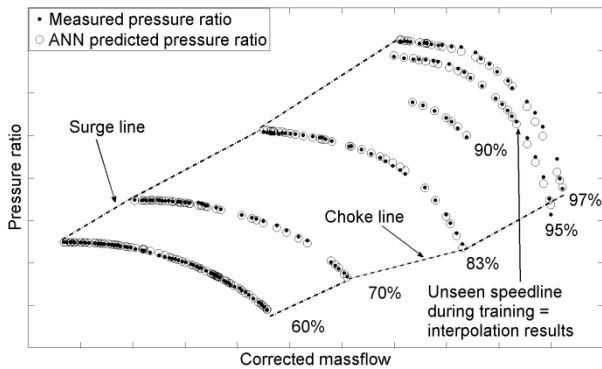
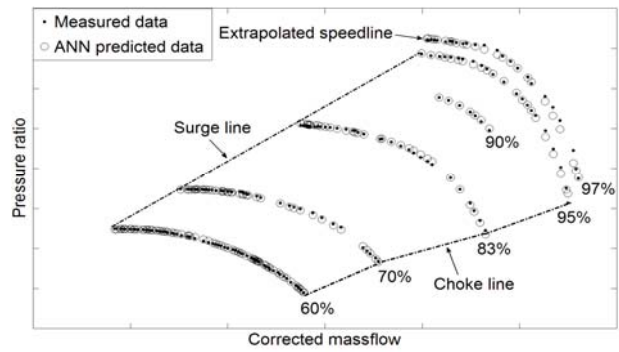


Fig. 4 Interpolation results for 95% speed line.

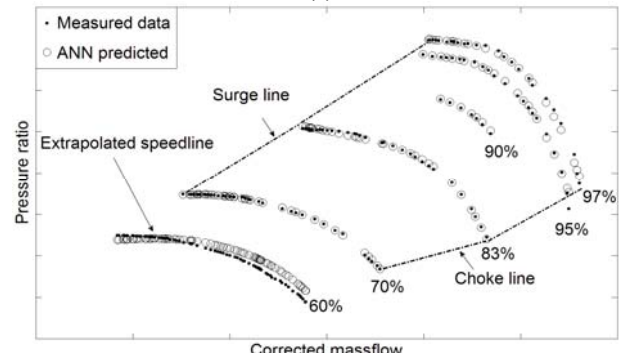
Table 2 Training and interpolation average error for each speed line.

Speed line	Error-interpolation (%)	Error-training (%)
60%	-	0.21
70%	0.23	0.22
83%	0.25	0.24
90%	0.26	0.26
95%	0.27	0.26
97%	-	0.25

average error for prediction of the 60% speed line is 0.7% and for 97% speed line 0.35%. The result is shown in Figs. 5a and 5b and it can be concluded that the extrapolation can be performed, however, as expected



(a)



(b)

Fig. 5 (a) Extrapolation results for 97% speed line; (b) extrapolation results for 60% speed line.

at reduced accuracy compared to interpolation. At least, the network seems to maintain the general behaviour of the shape of the speed line during extrapolation. The higher error for the 60% speed line can be explained by the fact that the network has to extrapolate a longer distance. This means that extrapolation should be, in the case it is necessary, applied to data close to the training data domain.

The previous models were trained with the existing data set, where each speed line is represented by several measurements close to each other. The question may arise how many data patterns actually are needed to model the compressor characteristics for pressure ratio prediction. This is dependent on several factors such as number of neurons in the model, number of input parameters as well as the shape of the function; a highly nonlinear function requires a higher number of data patterns than a simpler one. For that purpose, two test cases are investigated with the goal to quantify the minimum number of training data. In Case-1, three training data patterns and two cross validation patterns

evenly distributed along the speed line are used, while in Case-2, four data patterns and three cross validation patterns are used. The ANN models are constructed with three neurons in the hidden layer which was previously seen as enough for the given functional complexity between the input and output parameters. In Case-1, the data pattern per weight ratio is 1.7 while in Case-2, it is 2.3. The remaining data are used as test data to verify the generalisation performance. In Case-1, the average error in the test data is 0.46% and the result is shown in Figs. 6a and 6b.

The average error is higher than in the previous model where 206 data patterns were used in the training and it can be concluded that training data points are not enough to fully capture the compressor characteristic. However, in Case-2, see Figs. 7a and 7b, the average error in the test set is reduced to 0.25%, similar to when the 206 data patterns were used and it can be concluded that in this case the number of training data is enough to approximate the compressor characteristics.

6.2 Predicted Mass Flow— $\dot{m}_c = f(\pi_c, N_c)$

The compressor mass flow is predicted based on the normalized speed and the pressure ratio. The part of the speed lines that are almost horizontal in Model-I become almost vertical in Model-II which imply that this model is much more sensitive to small differences in pressure ratio than Model-I in compressor mass flow. A first attempt was made applying the same data normalisation scale as in Model-I, i.e. ± 0.8 . As indicated in previous studies [11], MLPs can not approximate the model except by drastically increasing the number of neurons. To exemplify this, Fig. 8 shows the network compressor characteristic approximated with four hidden neurons. The network fails to especially approximate the steep part of the speed lines and the error in the test data, applying a normalisation scale of ± 0.8 , is 1.1%.

This problem is related to the S-shaped transfer function in the neurons, the so-called basis functions. During training, the network weights are updated

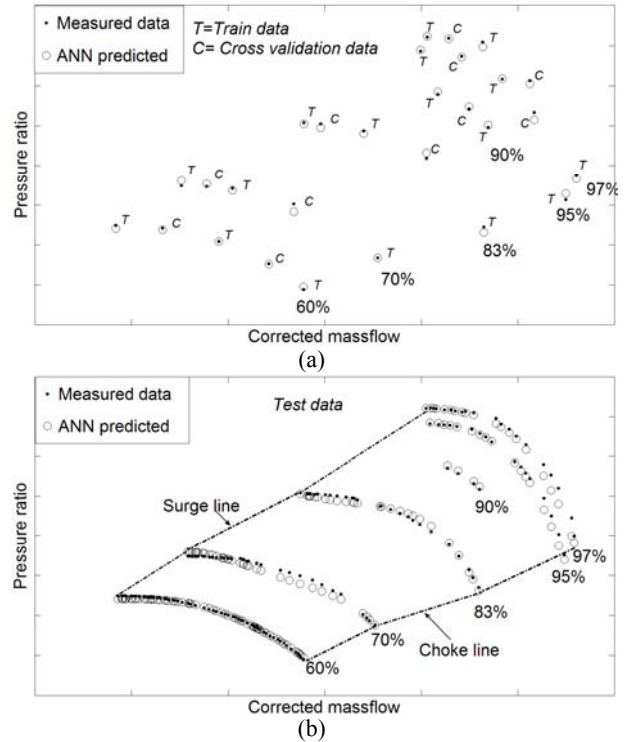


Fig. 6 (a) Case-1, training and cross validation data; (b) Case-1, test data.

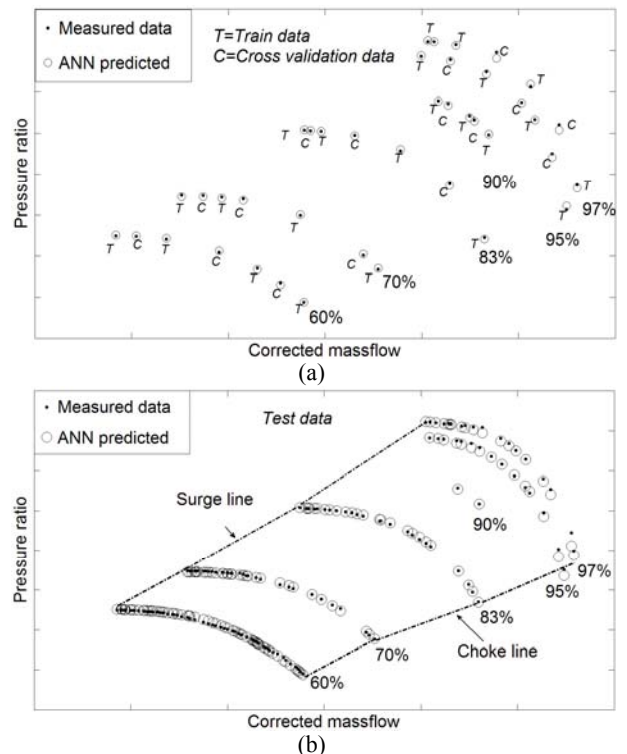


Fig. 7 (a) Case-2, training and cross validation data; (b) Case-2, test data.

which changes the actual shape of each basis function where each basis function is used to approximate a part

of the overall function, further discussion on this subject can be found in e.g. Ref. [17]. The main point is that different basis functions are used to obtain different parts of the approximated function, where one or several basis functions are used to obtain nonlinear approximations and others for the linear approximation. Because of this, it can be assumed that the optimal data normalisation scale partly depends on the function to be approximated. By applying a lower data normalisation scale, it will be easier for the ANN model to approximate the steep part of the approximated function, however, selection of a too low normalisation scale implies that the network will have difficulties to approximate the nonlinear part of the function. As recognized in Fig. 8, the function approximated in Model-II contains both a very steep part as well as a nonlinear part. It can be noted here that the difficulties for ANNs to approximate this type of functions have been reported in Ref. [8] where the authors applied ANN for compressor flow rate prediction as a function of pressure ratio and rotational speed of turbochargers.

The successful data normalisation scale was found to be at ± 0.4 , see Fig. 9 for the curve fitting result, where the average error in the test data set was 0.35%. Applying a lower data normalisation than ± 0.4 made the approximation of the nonlinear part difficult. The interpolation results are similar to the results obtained with Model-I. In contrary to the results obtained with Model-I, extrapolation was shown to yield totally useless predictions as shown in Fig. 10 for extrapolation of the 60% speed line. In summary, Model-II should specifically only be applied inside the training data domain.

6.3 Predicted Efficiency— $\eta_{mech} = f(n_c, \dot{m}_c)$

The estimated mechanical efficiency is calculated based on six different measured parameters, see Eq. (2), and because this is affected by noise in the measurements. Estimation of efficiency can be improved if the noise content in the measured parameters used to calculate the efficiency is reduced.

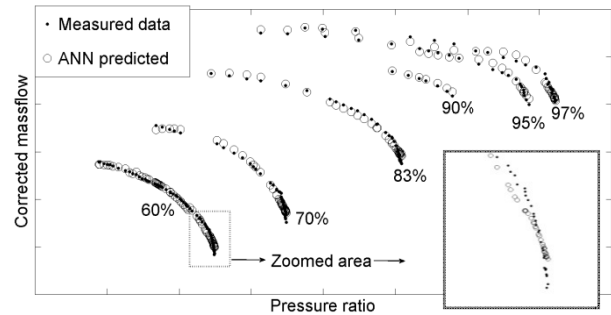


Fig. 8 Prediction of mass flow with a linear data normalisation scale of ± 0.8 .

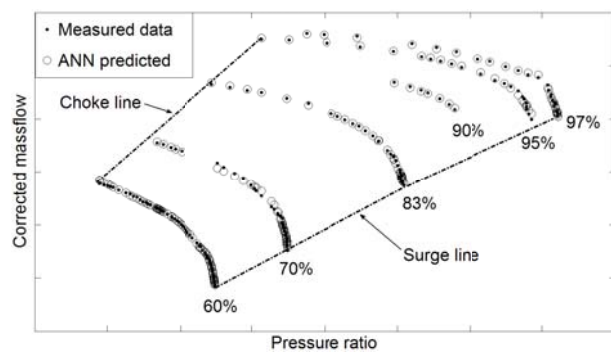


Fig. 9 Prediction of mass flow with a data normalisation scale of ± 0.4 .

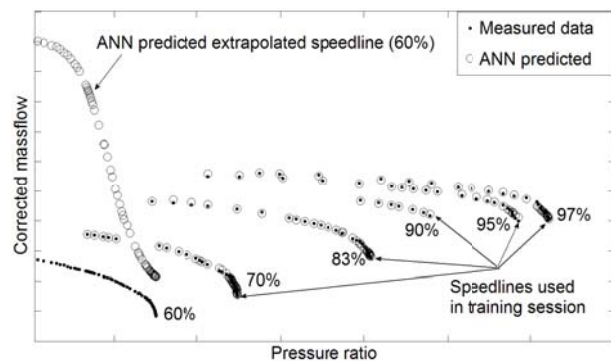


Fig. 10 Extrapolation result of the 60% speed line.

In this study, this is achieved by constructing one AANN network for each speed line and then use the AANN predicted values to recalculate the mechanical efficiency. The AANN networks are configured with a reduced dimension in the bottleneck layer which forces the network to learn the systematic interrelationship between the parameters while exclude uncorrelated information such as noise. The actual AANNs are configured with six neurons in the mapping layer and four neurons in the bottleneck layer, using a data set containing 1,020 data patterns. With this configuration, the network includes 155 weights

to be determined, in this case with a data pattern per weight ratio of 6.6. In Fig. 11, a schematic illustration of the data filtering process is shown, while Figs. 12a and 12b illustrate the noise reduction effect by the efficiency calculated with raw data and the efficiency calculated with the AANN filtered data. The efficiency calculated with raw data is rather scattered, while the efficiency calculated with AANN filtered data seems to be less scattered which indicates that noise filtering has been performed on the data when processed through the AANN model. It can also be noticed that the highest noise filtering effect is seen in the area where many measurement data points are located which shows how the AANN noise filtering capability depends on redundancy in the data. Fig. 12b

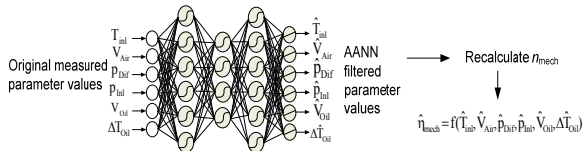


Fig. 11 Schematic illustration of the data noise filtering process.

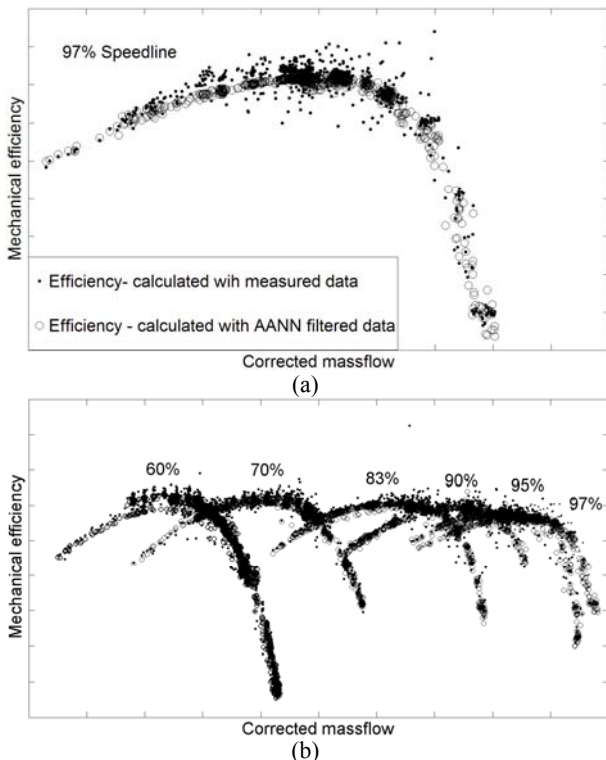


Fig. 12 (a) Calculated and AANN filtered efficiency, speed line 97%; (b) calculated and AANN filtered efficiency, all speed lines.

shows the result for all speed lines and Fig. 12a shows for speed line 97%. For all speed-lines, it can be clearly seen that the AANN processed data reduce the noise content. Because of this, the mechanical efficiency is calculated based on the filtered data prior to training of Model-III.

The AANN filtered data are used as the new training data for Model-III, where the final model needed four neurons in the hidden layer. The ANN model is trained in the same manner as the previous models, applying a linear data normalisation scale of ± 0.8 , similar as in Model-I. The average error for the mechanical efficiency is 0.55%. Fig. 13 shows the error as a function of number of neurons in the hidden layer and it can be recognized that three or four neurons is enough to approximate the input/output relationship. In Fig. 14, the prediction of mechanical efficiency by the ANN is shown together with the raw measurements. Interpolation and extrapolation was tested in Model-I with similar results, that meant interpolation was performed with similar accuracy as

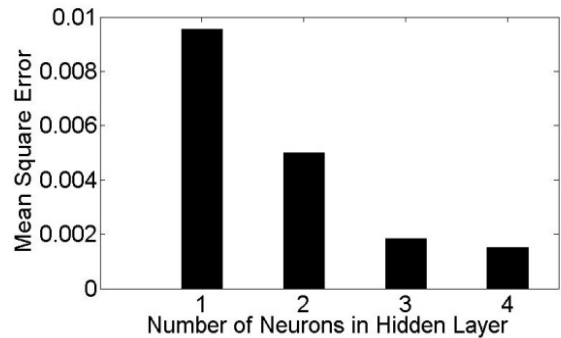


Fig. 13 Mean square error as a function of neuron.

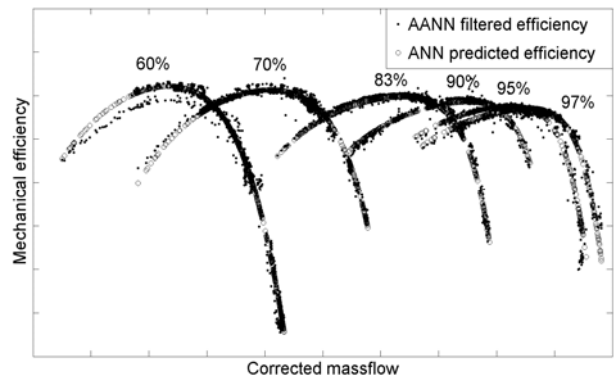


Fig. 14 Network prediction and measured mechanical efficiency.

in training data, while extrapolation could be performed at slightly increased error, in the case where data from 97% speed line was used for extrapolation. The error was similar to the training error while extrapolation of the 60% speed line results in an average error of 1.2%, approximately twice the training data error.

7. Conclusions

In this study, ANN models were used as curve fitting tools applied to measured data from an axial compressor test rig. Two specific objectives have been investigated, the first one targeting the optimal design parameters for ANN model configuration and development with respect to interpolation and extrapolation capabilities while the second objective was to evaluate the AANN for data screening and noise filtering purposes. For the curve fitting purpose, three different models were evaluated, prediction of pressure ratio, mass flow and mechanical efficiency. It was seen that for each model the compressor map could be approximated by a one hidden layer MLP with 3-4 neurons in the hidden layer, depending on the predicted parameter. All models revealed excellent interpolation capabilities and are in accordance to previous studies such as Ref. [8]. The compressor mass flow curve fitting model was the most challenging task since this required an unconventional data normalisation scale to provide acceptable data representation. Extrapolation was seen to be possible with acceptable results with Model-I and Model-III while Model-II revealed to provide unacceptable extrapolation prediction results. In summary, for compressor data curve fitting, Model-I and Model-III can be used for interpolation and to some extent extrapolation while Model-II should be restricted to interpolation, i.e. only be applied inside the training data domain. Comparing the results to similar studies, it was seen that simpler networks could be used than in Ref. [11], and the issue of mass flow prediction as reported in Ref. [8] is solved by applying lower data normalisation scale than normally used. The AANN

was applied as a pre-processing step to filter noise in the measured data used for mechanical efficiency calculation and a clear noise reduction was seen when the efficiency was calculated by the filtered data instead of the original measured data values. Thus, the AANN methodology can be used as a data cleaning tool, either to reduce the noise content in the data or to be used to select representative data points. In summary, the results in this study show that ANN can be used to develop efficient differentiable numerical models of the compressor characteristics when the data covering the main part of the operating window is available. In addition, some results regarding required number of data patterns as well as the needed number of neurons in the hidden layer for the different models are provided which can be useful for ANN modelling of compressors with similar characteristics.

References

- [1] A. Lazzaretto, A. Toffolo, Analytical and neural-network models for gas-turbine design and off-design simulation, *Int. J. Appl. Thermodyn.* 4 (4) (2001) 173-182.
- [2] H.I.H. Saravanamuttoo, B.D. MacIsaac, Thermodynamic model for pipeline gas-turbine diagnostics, *J. Eng. Power* 105 (3) (1983) 875-884.
- [3] P. Zhu, H.I.H. Saravanamuttoo, Simulation of an advanced twin-spool industrial gas-turbine, *Journal of Eng. Gas Turbine Power* 114 (1) (1992) 180-186.
- [4] J. Kurzke, How to get component maps for an aircraft gas-turbine's performance calculations, ASME Paper, Elissa, 1996.
- [5] G. Sieros, A. Stamatis, K. Mathioudakis, Jet engine component maps for performance modeling and diagnosis, *J. Propul Power* 13 (5) (1997) 665-674.
- [6] C.D. Kong, J. Ki, Components map generation of gas turbine engine using genetic algorithms and engine performance deck data, *J. Eng. Gas Turbines Power* 129 (2) (2007) 312-317.
- [7] C.D. Kong, S. Kho, J. Ki, Component map generation of a gas turbine using genetic algorithms, *J. Eng. Gas Turbines Power* 128 (1) (2006) 92-96.
- [8] P. Moraal, I. Kolmanovsky, Turbocharger modeling for automotive control application, SAE Transaction, 1999, pp. 1324-1338.
- [9] K. Ghorbanian, M. Gholamrezaei, Axial compressor performance map prediction using artificial neural network, in: ASME Conf. Proc., Montreal, Canada, 2007.

- [10] Y. Youhong, C. Lingen, S. Fengrui, W. Chih, Neural-network based analysis and prediction of compressor's characteristic performance map, *Applied Energy* 84 (2007) 48-55.
- [11] K. Ghorbanian, M. Gho lamrezai, An artificial neural network approach to compressor performance prediction, *Applied Energy* 86 (7-8) (2009) 1210-1221.
- [12] M.A. Kramer, Nonlinear principal component analysis using autoassociative neural networks, *AIChE Journal* 37 (2) (1991) 233-243.
- [13] P.J. Lu, T.C. Hsu, Application of autoassociative neural network on gas-path sensor data validation, *Journal of Propulsion and Power* 18 (4) (2002) 879-888.
- [14] K.U. Ziegler, K. Engel, P. Kufner, M. Engber, M. Ernst, R. Niehuis, On the need for thoroughly validated unsteady CFD in the aerodynamic optimization of aero engine compressors, *Cieplne Maszyny Przeplywowe Turbomachinery* 2 (128) (2005) 605-614.
- [15] M. Ernst, A. Michel, P. Jeschke, Analysis of rotor-stator-interactions and blade-to-blade measurements in a two stage axial flow compressor, *ASME Paper* 2009-GT-59371, 2009.
- [16] M.T. Hagan, M. Menhaj, Training feedforward networks with the Marquardt algorithm, *IEEE Transactions on Neural Network* 5 (6) (1994) 989-993.
- [17] C. Bishop, *Pattern Recognition and Machine Learning*, Springer, USA, 2006.